

Tomographic Site Characterization Using CPT, ERT and GPR¹

Rexford M. Morey (rmorey@ara.com; 802-763-8348)
Applied Research Associates, Inc.
RR1 120-A Waterman Road
South Royalton, VT 05068

Abstract

The integration of cone penetrometer logs (CPT) with electrical resistivity tomography (ERT) and ground penetrating radar (GPR) tomography increase the ability to characterize subsurface site conditions. Cross-hole ERT and GPR compliment each other. In regions of low resistivity ERT is more effective and in regions of high resistivity GPR is more effective. The three techniques, CPT, ERT and GPR, are briefly described and results are presented for an infiltration test to demonstrate imaging a salt water plume using pre-injection and post-injection tomograms. The test site consists of inter-bedded sand and clay layers that are imaged by both ERT and GPR. CPT soil stratigraphy logs and resistivity logs correlate well with the ERT and GPR results.

Introduction

The US Department of Energy (DOE) is responsible for the clean up of inactive DOE sites and for bringing DOE sites and facilities into compliance with Federal, State and local laws and regulations. Significant savings, in both time and money, can be realized with better site characterization and monitoring techniques. These techniques are required to better characterize the physical, hydrogeological, and chemical properties of the subsurface while minimizing and optimizing the use of boreholes and monitoring wells. Today the cone penetrometer technique (CPT) is demonstrating the value of a minimally invasive deployment system for site characterization.

Technologies used for site characterization and monitoring have numerous and diverse applications within site clean-up and waste management operations. There is a need for sensors, sensor deployment means, and sensor data processing, including sensor data fusion methodologies for:

- Detection and monitoring of contaminants in soils, groundwater, and process effluents;
- Expediting site characterization; and
- Geological and hydrogeological characterization and monitoring of the subsurface environment.

¹ Research sponsored by the U.S. Department of Energy's Federal Energy Technology Center, under contract DE-AR21-96MC33077. Contracting Officer's Representative is Karen L. Cohen, DOE/FETC.

Specific benefits are numerous where cost effective underground imaging is very important:

1. Delineating the continuity of soil layers between penetrometer holes;
2. Locating and mapping sand and clay lenses between penetrometer holes;
3. Mapping DNAPL plumes;
4. Defining spatial and temporal behavior of a steam flood for dynamic stripping;
5. Detecting leaks under tanks at Hanford, WA;
6. Monitoring the efficiency of air sparging;
7. Monitoring an ohmic heating thermal front;
8. Characterization of burial trenches and pits, including boundaries and contents; and
9. *In-situ* measurement of physical properties, i.e., porosity, density and moisture content.

CPT uses a variety of sensors for measuring soil properties, such as, pore pressure, resistivity, temperature, pH, and seismic wavespeed. Studies have shown that CPT site investigations at hazardous waste sites are a very cost-effective method for accessing the subsurface without drilling. Two new sensor packages for site characterization and monitoring have been developed for deployment with CPT. The two new CPT methods are:

- Electrical Resistivity Tomography (ERT) and
- Ground Penetrating Radar (GPR) Tomography.

Surface ERT and GPR have proven to be useful techniques for imaging subsurface structures and processes; however, depth of investigation is limited. Borehole use of ERT and GPR require the installation of system components via drilled boreholes. The installation of ERT electrodes and GPR antennas by cone penetrometer techniques reduces installation costs and total costs for ERT and GPR surveys. Using the cone penetrometer for environmental site characterization represents a new application of the technology. Significant advantages of the CPT include: eliminating drilling wastes and the need for treatment and disposal of drill spoils as hazardous material; reducing the possibility of cross contamination (by grouting the hole as the probe is withdrawn), and is faster than conventional drilling and sampling.

Technology Descriptions

Cone Penetrometer Technique

The cone penetrometer was originally developed in the Netherlands in 1934 for geotechnical site investigations. The original cones involved mechanical measurements of the penetration

resistance on a conical tip. A friction sleeve was added in 1965 (Begemann 1965). Electronic measurements were added in 1948 and improved in 1971 (de Reister 1971). Pore pressure probes were introduced in 1975 (Torstensson 1975; Wissa, et al. 1975), originally as independent probes, but were soon added to the cone penetrometer instrumentation. Modern CPT systems feature geotechnical sensors for tip stress, sleeve friction, pore pressure along with an inclinometer to measure the tilt of the probe, and resistivity and soil moisture sensors. This type of cone is primarily used for geotechnical investigations. However, the significant advantages CPT provides for environmental work is leading to much wider acceptance by the environmental site characterization community. This is due largely to the development of new sensors that allow detection of chemical pollutants in-situ.

Major components of the modern cone penetrometer system are the instrumented probe, the instrumentation conditioning and recording system, the hydraulic push system, and the vehicle on which the system is mounted. Enclosure in a van body allows all weather operation. The common configuration provides the reaction mass for a hydraulic push force of about 20 tons (18,000 kgs). Standardization for the geotechnical applications of the cone penetration test was established by the American Society of Testing and Materials in 1986. This standard allows for a probe diameter of 1.44 or 1.75 inches (3.658 cm or 4.445 cm). The most common for standard work is the 1.44-inch probe.

Recent environmental work, however, has led to the requirement to push deeper than possible with the 20 ton configuration. This has been accomplished by increasing the reaction weight to 30-35 tons (27,000 -32,000 kgs) and using the larger 1.75-inch probe and rod. This increases the rod buckling resistance at the higher loads. The maximum depth of penetration possible varies greatly with soil type. In soft damp soil, the 20-ton systems have penetrated 300 feet (91.5 m); but in gravelly soils, such as the Department of Energy's Hanford Site in southwestern Washington, these systems met refusal at 10-20 feet (3-6 m). A thirty-ton system using the larger diameter rods has reached depths of approximately 150 feet (46 m) in these same gravelly soils (Timian 1992).

Electrical Resistivity Tomography

In most environmental restoration applications the role of electrical resistivity is to assist in characterizing a site. The task includes not only specifying the location of contamination, but also mapping the physical and chemical properties of the ground that control their distribution and movement. In the most general sense, mapping electrical resistivity is important for conditioning or constraining the hydrological models of contaminant transport and retention. These models are usually based on drill-hole tests and suffer from the problem of extrapolation of point measurements to the volume between the holes.

For example, a channel of high permeability sand that is missed by a drill pattern illustrates the problem of relying solely on drill holes. This channel would be the dominant feature of the site

in terms of contaminant transport. Mapping the subsurface distribution of electrical resistivity could reveal the subsurface geometry and drastically change the hydrologic model.

Soil and rock resistivity (or conductivity) measurements have been used in the mining industry for many years, and recently have been used to monitor remediation of contaminate plumes (Daily and Ramirez 1995). The electrical resistivity of most soils and rocks depends on the conduction paths afforded by fluids in the pore spaces. The porosity, saturation, pore fluid salinity, and clay content determine resistivity. Because the dissolved solids in groundwater influence resistivity, mapping it may be the only direct detection method for high concentrations of contaminants that form ionic species.

ARA includes a Resistivity Module in its cone penetrometer instrumentation for measuring resistivity in the adjacent soil. As part of the CPT push rod, the module consists of four circular electrodes in contact with the soil. Insulators separate the electrodes. The outer two electrodes are used to induce an electrical current into the soil matrix. The inner two electrodes are used to measure the strength of the induced electric field. The amount of voltage potential drop in the electric field is a function of the resistivity of the soil.

Daily et al. (1992) and *Ramirez et al.* (1993) at the Lawrence Livermore National Laboratory, developed and tested the Electrical Resistivity Tomography (ERT) method for mapping subsurface conditions between boreholes. Applications included monitoring water movement in the vadose zone and monitoring an underground steam injection process for soil decontamination. ERT uses a dipole-dipole measurement technique, similar to those used in conventional surface resistivity surveys (Keller and Frischknecht 1966) to measure the bulk electrical resistivity distribution in the soil mass between two boreholes.

Taking measurements before the process is started and then repeating the measurements over time as the process proceeds can monitor processes such as steam injection. Each tomographic data set is then subtracted from the original background measurements to produce a “time lapse” image set of resistivity variations between the boreholes.

To image the resistivity distribution between two boreholes, several electrodes are placed in each hole, as shown in Figure 1. Each electrode must be in contact with the formation. A known current, I , drives two electrodes, and the resulting voltage difference, V , is measured between other electrode pairs. This process is repeated until all the linearly independent combinations are measured. Each voltage-to-current ratio is a transfer resistance. The goal is to calculate the distribution of resistivity in the vicinity of the boreholes given the measured transfer resistance.

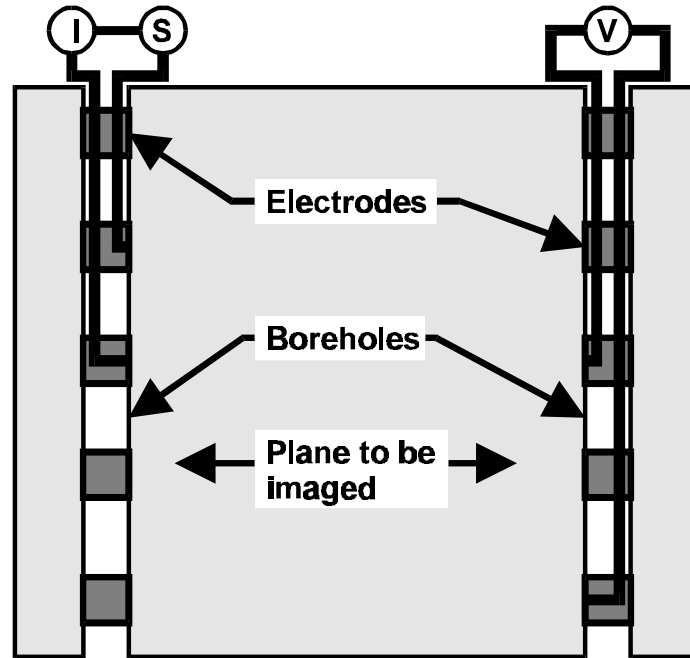


Figure 1. Schematic diagram showing data collection approach for ERT measurements.

The ERT image creation process involves solving both the forward and inverse problems. A finite element mesh, N elements wide (between the boreholes) and M elements long (along the boreholes) model the image reconstruction plane. Image resolution is a complicated function of many factors, including reconstruction pixel size, data signal-to-noise ratio, electrode and borehole separation, the subsurface resistivity distribution, and the degree to which the resistivity matches the two-dimensional model of the forward calculations. Resolution can be no better than one pixel; typical pixel size is 1 to 3 meters. The best resolution is obtained close to the electrodes, and the worst resolution is obtained along a vertical stripe midway between the boreholes. Thus, resolution improves as borehole spacing decreases.

Ground Penetrating Radar

Ground penetrating radar (GPR) has been used for over twenty years (Morey 1972; Daniels, et al. 1988) at chemical and nuclear waste disposal sites as a non-invasive technique for site characterization (Olhoeft 1992; Sandler, et al.1992). Standard GPR surveys are conducted from the surface of the ground providing geotechnical information from the surface to depths of 5 to 50 feet, depending on GPR frequency of operation and soil conductivity. Commercially available GPR systems operate over the frequency range 50 MHz to 1000 MHz. The lower frequencies provide better penetration but poor resolution, while the higher frequencies give poor penetration but good resolution. There are many critical environmental monitoring situations where surface GPR does not provide the depth of penetration or necessary resolution. Borehole radar (Bradley and Wright 1987) can place the sensor closer to the region of interest, overcoming the high signal attenuation in the near-surface soils.

Figure 2 is a schematic diagram showing possible data collection approaches for GPR measurements. These transmission measurements include hole-to-hole and hole-to-surface measurements. For cross-hole tomography (GPRT), one CPT antenna is held stationary while the other unit is moved. The process is repeated until the volume between the holes is covered. As the radar pulse propagates, it is attenuated due to conductivity and slowed due to the dielectric constant. Therefore, GPR tomography maps variations in conductivity and velocity from which it is possible to estimate soil characteristics, such as water content, density and contamination.

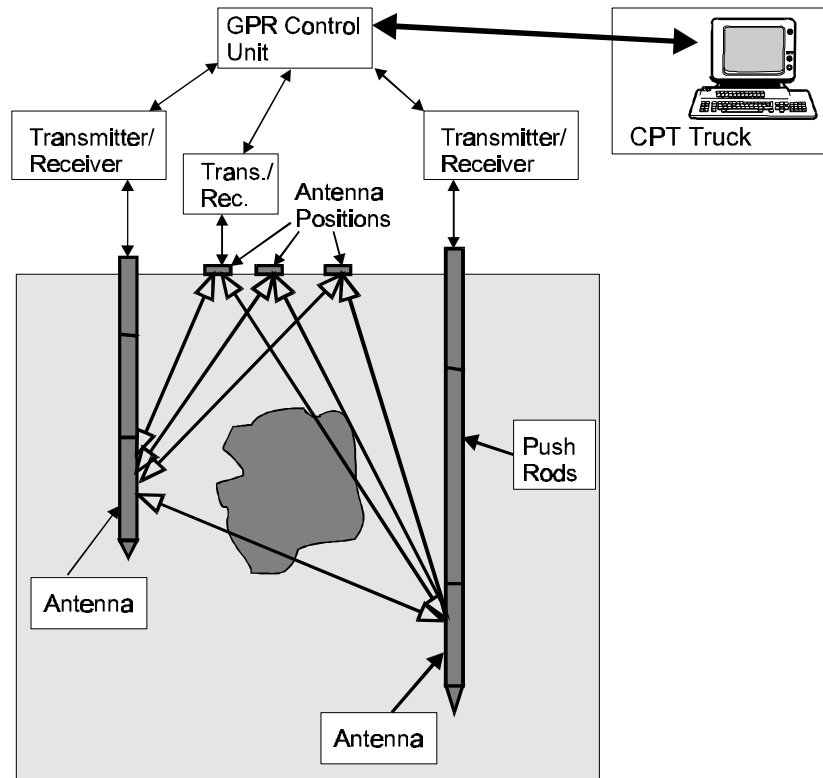


Figure 2. Schematic diagram showing data collection approach for GPRT measurements. Several ray paths are shown for typical transmitter-receiver positions on the surface and in the holes.

For GPRT data, a tomographic reconstruction is attempted using first-arrival times in an SIRT (simultaneous iteration reconstruction tomography) algorithm, initially with straight ray paths. However, if difficulty is experienced with convergence, then a perturbation method is used which allows for curved ray paths. The region under investigation is divided into a regular grid (similar to ERT) and the radar wavelet velocity and attenuation are iteratively calculated for each cell and combined to generate a map of the region between the holes. Spatial resolution is governed by the dominant wavelength of the pulses in the medium; at 100 MHz resolution is on the order of 0.5 to 1.5 meters.

Example Results

A test program was initiated at ARA's Vermont Test Site, near South Royalton, VT. Figure 3 shows the layout of GeoWells on the corners of a square with the infiltration well near the center of the square. CPT logs to a depth of 70 feet at each location delineate the soil stratigraphy, resistivity and pore pressure. Relatively thick layers of sand (10 to 15 feet) separated by thinner layers of clay and silty-clay (1 to 2 feet) characterize the site.

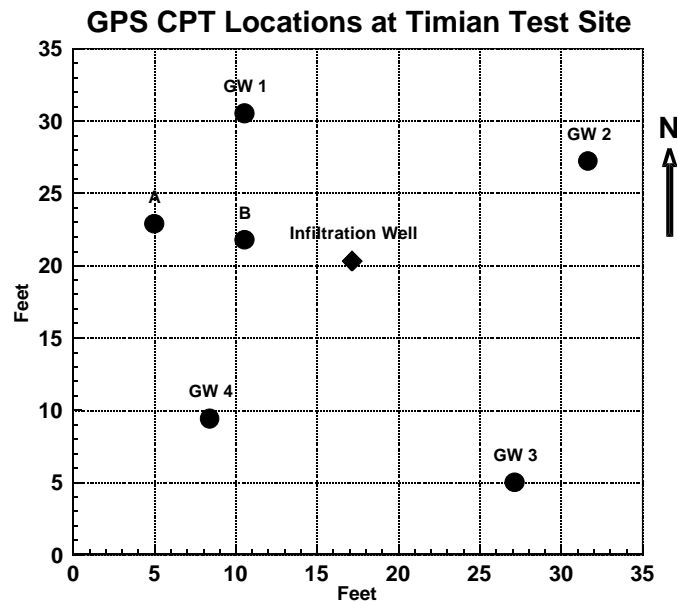


Figure 3. Relative location of GeoWells (GW) and infiltration well as determined from Global Position Satellite data. Wells A and B are monitoring wells.

The GeoWells are composed of sections of 2"-diameter PVC pipe with 10 ERT electrodes spaced 7' apart to a depth of 60 feet. About 100 gallons of saline water was injected in the 15-foot deep infiltration well. Both ERT and GPR cross-hole tomography data were taken from the GeoWells before and after the water injection.

Figure 4 is an example of an ERT tomogram between GeoWells 1 and 3 with the corresponding CPT resistivity log. Superimposed on the resistivity log are resistivity segments or layers calculated from the resistivity log data. Note the low resistivity at 38 feet and 50 feet in both the CPT log and the ERT image. Low resistivity occurs in the clay layers. ERT data above 20 feet was not usable because the soil was too resistive for adequate current injection.

An effective way of monitoring an ongoing process is to make a series of measurements over time and then display only the changes that occur. Figure 5 is an example of an ERT image

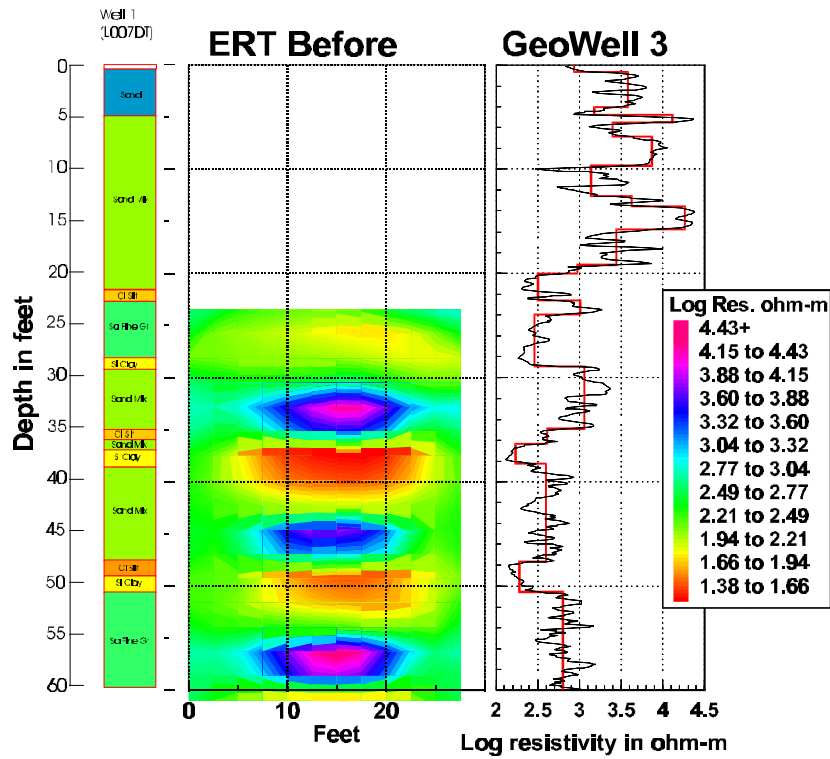


Figure 4. ERT tomograph, before injection of salt water. Included is the CPT resistivity log for GeoWell 3.

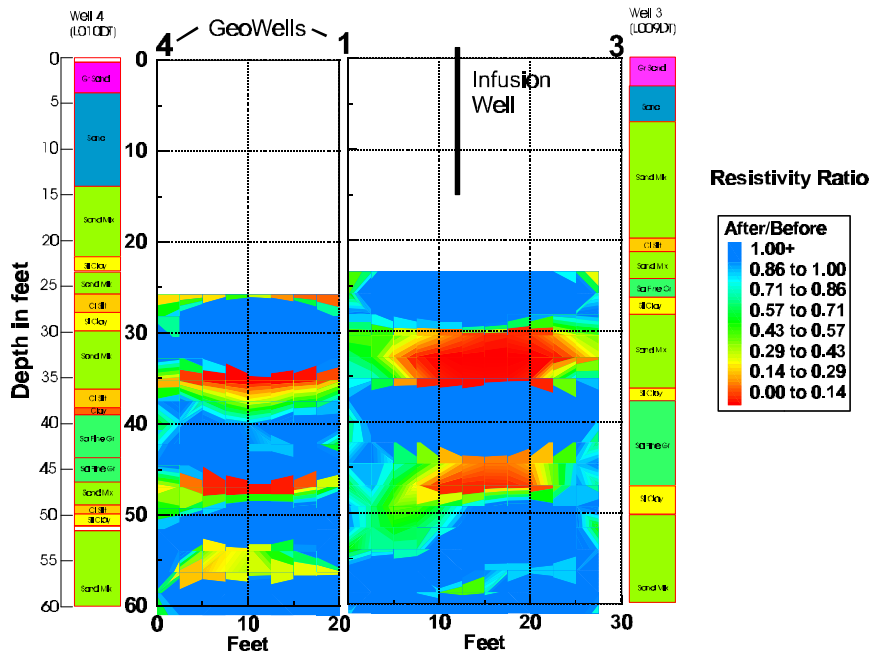


Figure 5. ERT image showing the difference between pre-injection and post injection results.

showing the difference between pre-injection and post-injection results. GeoWell 1 is common to the two panels (see Figure 3). The resistivity ratio is calculated by dividing the post-injection by the pre-injection data. The greatest changes (red) occur above the clay layers. The water plume seems to be moving along the top of the clay layers.

An example of GPR tomographic results is shown in Figure 6 for pre-injection and post-injection measurements.

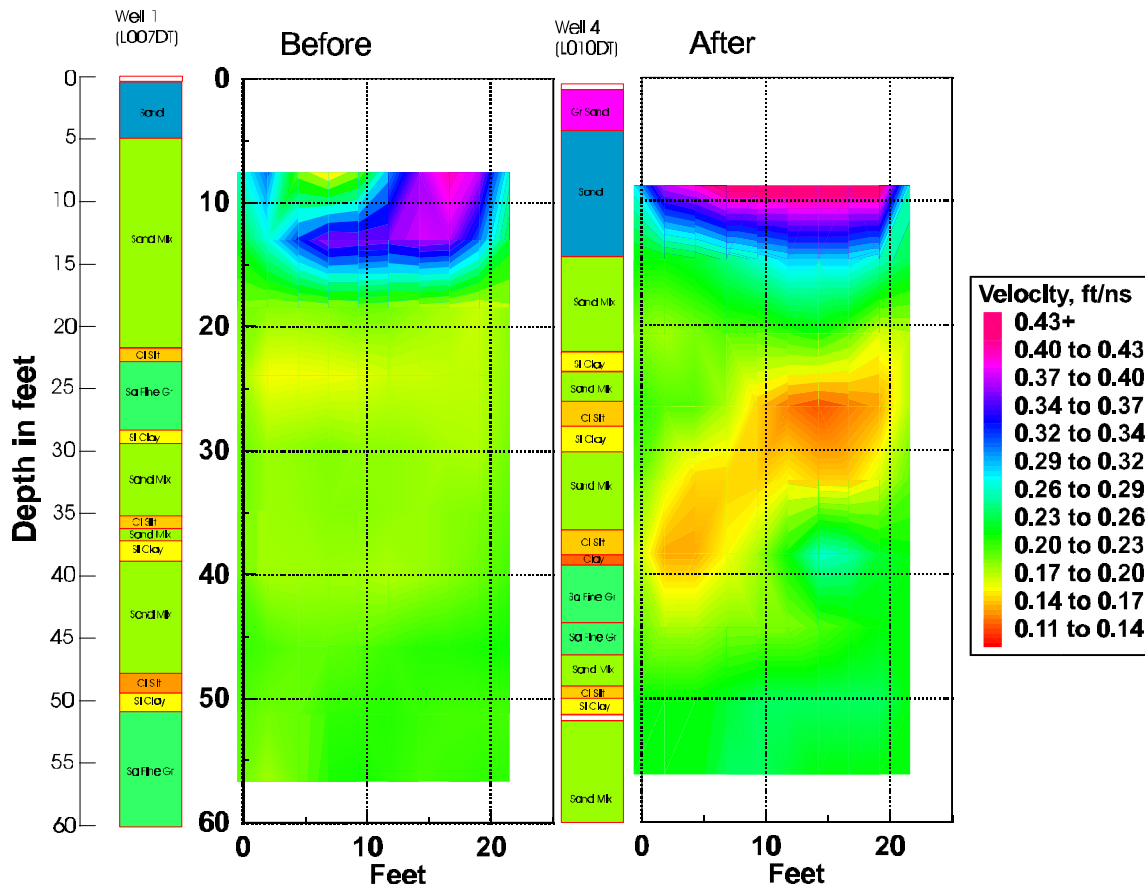


Figure 6. An example of GPR tomographic images between GeoWells 1 and 4 showing the results of pre-injection and post-injection data.

In the post-injection right panel the water plume extends from the upper right at about the 20-foot depth to the lower left at 40 feet. Post-injection measurements were made one day after the salt water was injected.

Conclusions

CPT methods can be used to install PVC/electrode GeoWells to a depth of 60-feet. The same GeoWells can be used to make both ERT and GPR cross-hole measurements. ERT and GPR tomographic images will show the migration of a salt-water plume in inter-bedded sand and clay formations.

References

- Begemann, H. K. S., 1965. "The Friction Jacket Cone as an Aid in Determining the Soil Profile," *Proc. 6th ICSMFE*, Montreal, vol. I, pp. 17-20.
- Bradley, J. A., and D. L. Wright, 1987. "Microprocessor-Based Data-Acquisition System for a Borehole Radar," *IEEE Trans. Geosci. Remote Sensing*, vol. GE-25, pp. 441-447.
- Daily, W., A. Ramirez, D. LaBrecque, and J. Nitao, 1992. "Electrical resistivity tomography of vadose water movement," *Water Resources Research*, vol. 28, pp. 1429-1442.
- Daily, W. and A. Ramirez, 1995. "Electrical resistance tomography during in-situ trichloroethylene remediation at the Savannah River Site," *Journal of Applied Geophysics*, 33, pp. 239-249.
- Daniels, D. J., D. J. Gunton, and H. F. Scott, 1988. "Introduction to subsurface radar," *IEE Proceedings on Communication, Radar, and Signal Processing*, vol. 135, Pt. F, pp. 278-320.
- de Reister, J., 1971. "Electric Penetrometer for Site Investigations," *Journal of SMFE Division*, ASCE, vol. 97, SM-2, Feb. pp. 457-472.
- Keller, G. V., and M. Frischknecht, 1966. *Electrical Methods in Geophysical Prospecting*, Pergamon, New York.
- Morey, R. M., 1974. "Continuous Subsurface Profiling by Impulse Radar," *Proceedings of the Engineering Foundation Conference on Subsurface Exploration*, Henniker, NH, American Society of Civil Engineers, pp. 213-232, August.
- Olhoeft, G. R., 1992. "Geophysical Detection of Hydrocarbon and Organic Chemical Contamination," in *Proc. Symposium on the Application of Geophysics to Engineering and Environmental Problems*, pp. 587-595, April 26-29, Chicago, IL.
- Ramirez, A., W. Daily, D. LaBrecque, E. Owen, and D. Chesnut, 1993. "Monitoring an Underground Steam Injection Process Using Electrical Resistivity Tomography," *Water Resources Research*, vol. 29, pp. 73-87.
- Sander, K. A., G. R. Olhoeft, and J. E. Lucius, 1992. "Surface and Borehole Radar Monitoring of a DNAPL Spill in 3D versus Frequency, Look Angle and Time," in *Proc. Symposium on the Application of Geophysics to Engineering and Environmental Problems*, pp. 455-469, April 26-29, Chicago, IL.
- Timian, D. A., B. E. Fisk, and B. R. Cassem, 1992. "Demonstration of Heavyweight Penetrometer Technology at the Hanford Site," *WHC-SD-TRP-003*, Westinghouse Hanford Company, Richland, Washington, December.
- Torstensson, B. A., 1975. "Pore Pressure Sounding Instrument," *Proc. ASCE Spec. Conf. on In Situ Measurement of Soil Properties*, Raleigh, NC, vol. II, pp. 48-54.
- Wissa, A. E. Z., R. T. Martin, and J. E. Garlanger, 1975. "The Piezometer Probe," *Proc. ASCE Spec. Conf. on In Situ Measurement of Soil Properties*, Raleigh, NC, vol. I, pp. 536-545.